Catalysis Communications 16 (2011) 45–49

Contents lists available at SciVerse ScienceDirect

Catalysis Communications

journal homepage: www.elsevier.com/locate/catcom

Short Communication

# Efficient synthesis of dimethyl carbonate via transesterification of ethylene carbonate with methanol over binary zinc-yttrium oxides

Liguo Wang [a,b], Ying Wang [a,b], Shimin Liu [a,b], Liujin Lu [a], Xiangyuan Ma [a], Youquan Deng [a,*]

[a] Centre for Green Chemistry and Catalysis, Lanzhou Institute of Chemical Physics, Chinese Academy of Sciences, Lanzhou 730000, China
[b] Graduate University of Chinese Academy of Sciences, Beijing 100039, China

ARTICLE INFO

*Article history:*
Received 28 June 2011
Received in revised form 25 August 2011
Accepted 6 September 2011
Available online 14 September 2011

*Keywords:*
Dimethyl carbonate
Ethylene carbonate
Transesterification
Binary zinc–yttrium oxide

ABSTRACT

The binary zinc–yttrium oxides were prepared by co-precipitation method, characterized and tested in the synthesis of DMC via transesterification of ethylene carbonate with methanol. The catalytic results showed that the catalyst with Zn/Y molar ratio of 3 and calcined at 400 °C exhibited superior catalytic activity, corresponding to TOF of 236 mmol/$g_{cat}$ h. Appropriate content of yttrium in the catalyst enhanced the catalytic activity remarkably. Moreover, the abundance of medium basic sites ($7.2 < H_- < 9.8$, as determined by Hammett indicator method) was considered to be responsible for the superior catalytic activity.



## 1. Introduction

As the lowest homologue in the family of dialkyl carbonates, dimethyl carbonate (DMC) has drawn specific attention as a non-toxic and environmentally friendly building block for a variety of chemicals [1]. DMC is a promising substitute for phosgene in the syntheses of aromatic polycarbonates [2], carbamates [3], isocyanates [4], etc. As a safe and environmental-friendly alternative, it can be also used as alkylation reagent for carbon, nitrogen, oxygen and sulfur centers [5]. Additionally, DMC has potential applications in the fields of fuel additive [6], lithium batteries electrolyte [7].

The industrial manufacture of DMC via phosgenation [8] and oxidative carbonylation of methanol [9] involved high-risk compounds of $COCl_2$ and CO. The chemical utilization of $CO_2$ as the raw material to synthesize useful chemical feedstocks has drawn much attention in recent years [10–12]. The production of DMC via transesterification of cyclic carbonates with methanol was a suitable synthetic pathway because the syntheses of raw material cyclic carbonates, such as ethylene carbonate (EC), propylene carbonate, from epoxides and carbon dioxide were well established [10, 11]. Therefore, the transesterification route aforementioned has the merits of cleanness and high efficiency for indirect utilization of $CO_2$ to synthesize DMC. It should be noted that DMC can also be synthesized via one-pot reaction directly from epoxides, $CO_2$ and methanol [13, 14], however, undesired side reaction such as ring opening of epoxides by methanol led to relatively lower DMC selectivity.

Over the past decades many efforts were devoted for synthesizing DMC via transesterifcation of cyclic carbonates with methanol, and several homogenous or heterogeneous catalytic systems have been reported previously, such as Mg–Al-hydrotalcite [15], Fe–Zn double metal cyanide [16], semectite [17], mesoporous CaO–$ZrO_2$ nano-oxides [18], activated dawsonites [19], polymer [20], or Au/$CeO_2$ [21]. However, most catalytic systems suffer from low catalytic activity, high reaction temperature or involvement of noble metals. Therefore, the development of an effective and stable heterogeneous catalyst is still highly desirable for this important process due to the significance both in fundamental research and industrial manufacture. The reaction is shown in Scheme 1.

In this study, binary zinc–yttrium oxides were prepared by co-precipitation method. These catalytic materials were found to catalyze the DMC synthesis from EC and methanol with high efficiency. The catalysts were characterized by means of nitrogen adsorption, XRD, XPS, FE-SEM, and Hammett indicator methods in detail. Influence of the preparation parameters (Zn/Y molar ratio, catalyst activation), and the effect of reaction parameters (MeOH/EC, reaction time) were also investigated in a batch mode.

## 2. Experimental

### 2.1. Materials

$Zn(OAc)_2 \cdot 2H_2O$ and $Y(NO_3)_3 \cdot 6H_2O$ were both of analytical grades, and were purchased from Sinopharm Chemical Reagent Co., Ltd.

* Corresponding author.
*E-mail address:* ydeng@licp.cas.cn (Y. Deng).

1566-7367/$ – see front matter © 2011 Elsevier B.V. All rights reserved.
doi:10.1016/j.catcom.2011.09.004

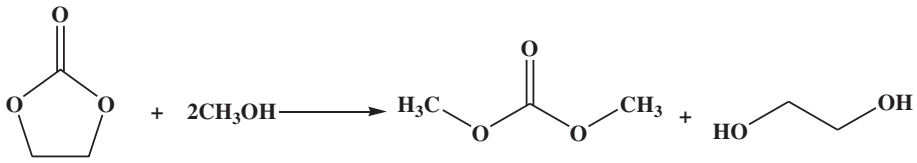


**Scheme 1.** Transesterification of ethylene carbonate and methanol to dimethyl carbonate.

### 2.2. Catalyst preparation

A mixture of given amount of $Zn(OAc)_2 \cdot 2H_2O$ and $Y(NO_3)_3 \cdot 6H_2O$ in designated ratios was dissolved into distilled water under stirring. Subsequently, 1 M aqueous solution containing sodium hydroxide and sodium carbonate was added dropwise until the pH of mixed solution reached 11. The resulting precipitate then was aged, filtrated, washed, and calcined in static air for 4 h. The obtained white solid was denoted as $Zn_xY$-T, where the x represents the Zn/Y molar ratio, and T is the calcination temperature.

### 2.3. Catalyst characterization

$N_2$ adsorption and desorption isotherms at 77 K were measured on a Micromeritics ASAP 2010 surface analyzer.

Powder X-ray diffraction (XRD) was measured on a Siemens D/max-RB powder X-ray diffractometer.

X-ray photoelectron spectroscopy (XPS) analysis was performed with a VG ESCALAB 210 instrument.

The morphological structures of the zinc–yttrium precipitate and the ones calcined at the temperature region of 300–600 °C were examined by field emission scanning electron microscopy (FE-SEM, JSM-6701F).

Hammett indicator method was used to measure the basic strength distribution of the catalyst according to the literature [22]. In a typical measurement, a mixture of 50 mg catalyst and 5 ml dry methanol was stirred for 2 h and the resultant solution was titrated against the standard benzene carboxylic acid solution.

### 2.4. Catalytic testing

In a typical reaction procedure, 2.64 g EC (30 mmol), 7.6 g methanol (240 mmol) and 0.07 g binary zinc–yttrium oxide catalyst (2.5 wt.% respect to the amount of EC) were added into a 50 ml flask. The reaction mixture was heated up to 65 °C and the reaction was conducted at atmospheric pressure. After the completion of reaction, the catalyst was recovered by centrifugation, and the quantitative analysis of the product was determined by Agilent 6820 GC (FTD detector) with octane as internal standard.

## 3. Results and discussion

### 3.1. Catalyst characterization

#### 3.1.1. Nitrogen physisorption

The textural properties for the binary zinc–yttrium oxides were shown in Table 1. The higher BET surface area of 182.5 $m^2/g$ could be obtained when the sample calcined at 400 °C is compared to that of 300 or 600 °C. On the other hand, relatively lower pore volume and diameter size were obtained simultaneously. It indicated that the calcination temperature had a strong influence on the catalyst textures. Notably, with this preparation method, catalytic materials with relatively high surface area and mesostructured pores could be obtained.

**Table 1**
Textural properties of the binary zinc–yttrium oxides as a function of calcination temperature.

| Catalyst | $S_{BET}$ ($m^2/g$) | P ($cm^3/g$) | d (nm) |
|---|---|---|---|
| $Zn_3Y$-300 | 65.7 | 0.232 | 10.2 |
| $Zn_3Y$-400 | 182.5 | 0.108 | 2.4 |
| $Zn_3Y$-600 | 20.5 | 0.107 | 17.9 |

#### 3.1.2. Crystal structure

The X-ray diffractograms of the ZnO, $Y_2O_3$ and $Zn_3Y$ binary oxides are shown in Fig. 1. Diffractograms of $Y_2O_3$ sample mainly consisted of amorphous phase, and poorly crystalline body-centered cubic yttrium oxide was identifiable (JCPDS 89–5592). The diffractograms for ZnO were dominated by hexagonal structure of crystalline zinc oxide (JCPDS 89–1397). In contrast, the intensities of XRD lines specific to $Y_2O_3$ in the $Zn_3Y$-400 binary oxide were higher than that of pure $Y_2O_3$, suggesting the involvement of zinc element improves the crystallization of $Y_2O_3$. The characteristics of $Y_2O_3$ peaks became sharper with increase of calcination temperature or after reuse for six times. It suggested that the higher calcination temperature and calcination procedure between each recycling run to regenerate the catalytic activity promoted the crystallization of $Y_2O_3$, which was also consistent with the view in reference [23].

#### 3.1.3. XPS analysis

The chemical state and surface composition of the $Zn_3Y$ samples as a function of calcination temperature are shown in Table 2. The peaks with binding energy (BE) located at 1021.7, 156.3–157.9, 529.3 and 531.3 eV can be attributed to Zn $2p_{3/2}$, Y 3 $d_{5/2}$, $O_{1at}$ 1 s (lattice oxygen) and $O_{ad}$ 1 s (adsorbed oxygen), respectively. BE of Y 3 $d_{3/2}$ gradually shifts from 157.9 to 156.3 eV with calcination temperature increased from 300 to 600 °C. The shift toward lower BE value indicated that $Y^{3+}$ ionic state possessed enhanced electron density with the increase of calcination temperatures, and a possible reason was that the electron transfer from oxygen vacancy to metal atoms of yttrium probably occurred as reported in the literature [24]. Percentage of the surface lattice oxygen ($O_{lat}$), or together with $Zn^{2+}$ and $Y^{3+}$ as total amount both reached maximum for the sample calcined at 400 °C. The concentration of $O_{lat}$ species decreased with further elevating calcination temperature to 500 or 600 °C. Subsequently, the concentrations of the $O_{lat}$ follow the order: $Zn_3Y$-400 > $Zn_3Y$-500~$Zn_3Y$-600 > $Zn_3Y$-300.

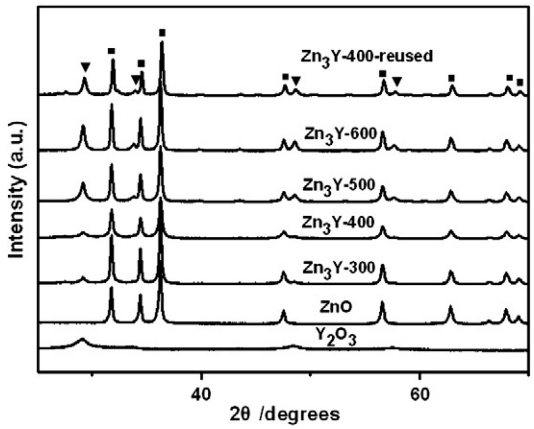


**Fig. 1.** Power XRD patterns of $Y_2O_3$, ZnO, and binary zinc–yttrium oxide samples. (■) Hexagonal phase of ZnO. (▼) Body-centered cubic phase of $Y_2O_3$.

**Table 2**
Binding energies of core electrons and XPS atomic ratios of binary zinc–yttrium oxides as a function of calcination temperature.

| Samples | Binding energy (eV) | | | | Surface percentage (at.%) | | | Surface atom ratio of $O_{lat}$/($Zn^{2+}+Y^{3+}$) |
|---|---|---|---|---|---|---|---|---|
| | $Y3d_{3/2}$ | $O_{lat}$ | $O_{ad}$ | $Zn2p_{1/2}$ | $O_{lat}$ | $Zn^{2+}$ | $Y^{3+}$ | |
| $Zn_3Y$-300 | 157.9 | 529.2 | 531.4 | 1021.7 | 4.2 | 9.1 | 6.4 | 0.27 |
| $Zn_3Y$-400 | 157.5 | 529.3 | 531.5 | 1021.6 | 9.4 | 21.6 | 11.3 | 0.22 |
| $Zn_3Y$-500 | 156.5 | 529.3 | 531.3 | 1021.7 | 5.6 | 15.0 | 9.3 | 0.39 |
| $Zn_3Y$-600 | 156.3 | 529.4 | 531.3 | 1021.6 | 5.8 | 10.6 | 0.6 | 0.52 |

**Table 3**
Base strength (H_) distribution obtained from Hammett indicator measurements.

| Entry | Catalyst | Basicity (mmol/$g_{cat.}$) | | | |
|---|---|---|---|---|---|
| | | 4.2<H_<7.2 | 7.2<H_<9.8 | H_>9.8 | Total |
| 1 | ZnO | 0.13 | 0.21 | – | 0.34 |
| 2 | $Y_2O_3$ | 0.04 | 0.19 | – | 0.23 |
| 3 | $Zn_3Y$-300 | 0.10 | 0.31 | 0.48 | 0.89 |
| 4 | $Zn_3Y$-400 | 0.89 | 0.74 | 0.18 | 1.81 |
| 5 | $Zn_3Y$-500 | 0.37 | 0.46 | 0.19 | 1.02 |
| 6 | $Zn_3Y$-600 | 0.29 | 0.37 | 0.14 | 0.80 |

### 3.1.4. Basicity characterization

The effect of the calcination temperature on the basicity was determined by Hammett indicator method (Table 3). Apparently, the higher total amount of basicity was obtained for the binary metal oxide compared to the corresponding single metal oxide, suggesting that the surface basicity was improved through combing the two components of zinc and yttrium. Among the binary oxides, the one calcined at 400 °C with the larger surface area possessed more total basic sites (1.81 mmol/g), simultaneously with the amount of medium basicity ($7.2 \leq H\_ \leq 9.8$) up to 0.74 mmol/$g_{cat}$. Additionally, the concentration of the medium basic sites follows the trends: $Zn_3Y$-400>$Zn_3Y$-500>$Zn_3Y$-600>$Zn_3Y$-300. In association of the XPS results, it can be found that the concentration sequence of the medium basic sites is essentially consistent with that of the $O_{lat}$ species. For metal oxides, lattice oxygens on the surface are generally considered to act as Lewis base sites [25]. Therefore, it can be proposed that the $O_{lat}$ species plays an important role in the Lewis basicity.

### 3.1.5. SEM study

The representative morphology of $Zn_3Y$ precipitate and morphology evolution of $Zn_3Y$ samples along with the increase of calcination temperature (300–600 °C) were studied by means of FE-SEM, as shown in Fig. 2. The $Zn_3Y$ precipitate exhibits hexagonal rod-like morphology. Upon calcination at 300 °C, the morphology with the poriform and discriminable sheet-like features were observed. Interestingly, after calcining the precursor at 400 °C, the resulting $Zn_3Y$-400 sample primarily consists of nanostructured sheet-like morphology with the thickness ~100 nm. By contrast, the compact aggregated palates with irregular size were observed after calcination at higher temperature of 600 °C, suggesting that the grains sintered to form the larger particles. In brief, besides the uncalcined catalyst with hexagonal rod-like morphology, the calcination of the catalyst precursor at varied temperatures resulted in different morphologies, but not prominent.

## 3.2. Catalytic testing

The transesterification of EC and methanol for DMC synthesis was investigated over various catalysts (Table 4). 11–19% of EC conversions with 10–17% of DMC yields were obtained over $Y_2O_3$ and ZnO catalysts, entries 1–2. For conciseness, the catalytic activity was expressed in the form of DMC yield in the following discussion. For the physical mixed oxide, entry 3, it exhibited 13% of DMC yield. Additionally, when $Zn_3Y$ precipitate was employed, it was almost inactive to the DMC synthesis, entry 4. Among the catalysts calcined at different temperatures, entries 5–8, $Zn_3Y$-400 exhibited 54% of DMC yield with 51% of slightly lower EG yield, corresponding to higher TOF of 236 mmol/$g_{cat}$ h compared to previous reports [15–21]. It indicated that 400 °C was the proper activation temperature for obtaining better catalytic activity. Higher catalytic activity was obtained over binary zinc–yttrium oxide than that of the physical mixture. This result demonstrated

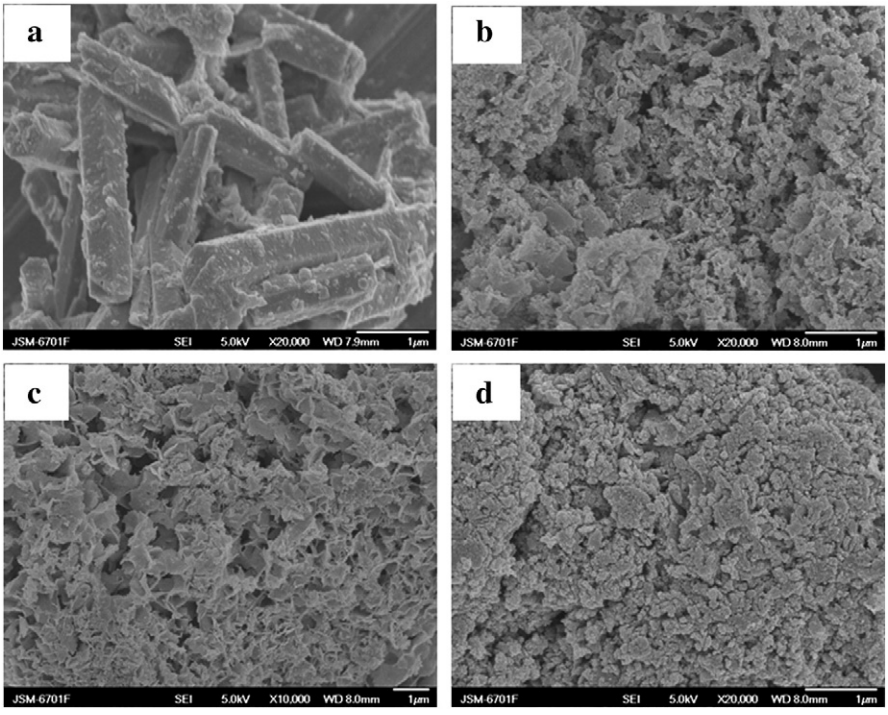


**Fig. 2.** FE-SEM images of (a) $Zn_3Y$ precipitate, (b) $Zn_3Y$-300, (c) $Zn_3Y$-400 and (d) $Zn_3Y$-600.

**Table 4**
Results of transesterification of EC and methanol over various catalysts.

| Entry | Catalyst | EC Con./% | DMC Yield./% | EG Yield./% |
|---|---|---|---|---|
| 1 | $Y_2O_3$ | 11 | 10 | –[c] |
| 2 | ZnO | 19 | 17 | 16 |
| 3[a] | ZnO–$Y_2O_3$ | 16 | 13 | 12 |
| 4[b] | $Zn_3Y$-uncalcined | 8 | 5 | – |
| 5 | $Zn_3Y$-300 | 33 | 31 | 30 |
| 6 | $Zn_3Y$-400 | 55 | 54 | 51 |
| 7 | $Zn_3Y$-500 | 48 | 45 | 42 |
| 8 | $Zn_3Y$-600 | 46 | 41 | 38 |
| 9 | ZnY-400 | 38 | 34 | 30 |
| 10 | $Zn_4Y$-400 | 46 | 44 | 43 |
| 11[d] | $Zn_3Y$-400 | 34 | 33 | 33 |

Reaction conditions: EC, 30 mmol; methanol, 240 mmol; catalyst, 0.07 g; 65 °C; 1 h; a: 0.07 g physically mixed ZnO and $Y_2O_3$ (molar ratio of Zn/Y = 3/1); b: $Zn_3Y$ precipitate; c: not detectable. d: 20 °C.

that the integration of zinc and yttrium components can remarkably improve the catalytic activity and the synergistic effect between them probably occurred. In some cases reported in the previous literatures [26, 27], it was demonstrated that the catalytic materials with different morphologies exhibited distinct catalytic performance through exposing various reactive crystal planes. However, in association of the basicity and FE-SEM characterizations, it can be seen that the catalysts investigated without prominent differences in morphology exhibited distinct variation in catalytic activity, i.e. 31% and 54% DMC yields for $Zn_3Y$-300 and $Zn_3Y$-400, respectively. It also can be found that the catalytic sequence is essentially consistent with that of medium basicity ($7.2 < H_- < 9.8$, as determined by Hammett indicator method). Generally, it was widely accepted that transesterification reaction was efficiently catalyzed by acid–base catalysts [28]. Therefore, it is reasonable to infer that the medium basic sites on the catalyst surface have a vital influence on the catalytic activity, i.e. $Zn_3Y$-400 with more medium basic sites demonstrated higher catalytic activity. Moreover, considering the relationship between the medium basicity and oxygen species, Lewis basic sites of $O_{lat}$ probably acted as the active sites.

Binary zinc–yttrium oxides with other molar ratio of Zn/Y, such as 1 or 4, were also tested, entries 9–10. However, lower DMC yields were obtained, especially obvious for the catalyst with Zn/Y molar ratio of 1, entry 9. It indicated that appropriate content of yttrium in the catalyst was more effective for the DMC synthesis. That is, there was an optimum composition of the catalyst for obtaining higher catalytic activity and the catalyst with molar ratio of Zn/Y 3 was most active. Notably, the catalyst exhibited 33% of DMC yield at 20 °C, entry 11, suggesting the catalyst was active even at room temperature condition.

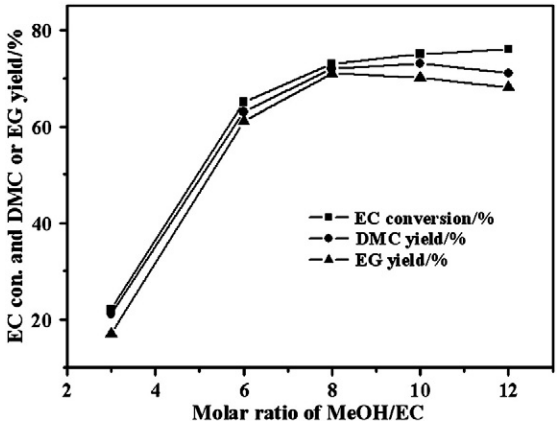


**Fig. 3.** The effect of MeOH/EC on the catalytic synthesis of DMC. Reaction conditions: 30 mmol EC; 0.07 g $Zn_3Y$-400; 2 h; 65 °C.

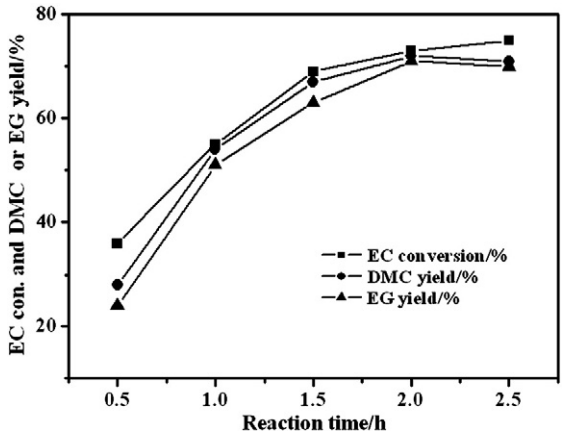


**Fig. 4.** The effect of reaction time on the catalytic synthesis of DMC. Reaction conditions: 30 mmol EC; 240 mmol methanol; 0.07 g $Zn_3Y$-400; 65 °C.

The influence of MeOH/EC molar ratio on DMC synthesis in the range of 3–12 was also investigated, as shown in Fig. 3. A significant increase in DMC yield was observed when the MeOH/EC molar ratio increased from 3 to 6, and reached the maximum when the ratio was 8. Further increasing the molar ratio did not improve the DMC yield apparently within 2 h reaction time. The dependence of DMC synthesis on the reaction time was also investigated in the range of 0.5–2.5 h, as shown in Fig. 4. A maximum DMC yield of 72% could be obtained within 2 h. Further prolonging the reaction time has no positive effect in increasing the DMC yield, indicating that the reaction reached the equilibrium.

### 3.3. Recyclability of the catalyst

The recycling test for the catalyst was shown in Fig. 5. After a simple calcination at 350 °C, the catalytic activity can be essentially regenerated. The catalyst can be reused without significant loss in activity in the subsequent runs, and 65% of DMC yield could be obtained even after six runs. The preservation of the crystal structure measured by XRD characterization was considered to be partially responsible for the good recyclability.

## 4. Conclusions

In summary, binary zinc–yttrium oxides were prepared by co-precipitation method and $Zn_3Y$-400 was found to be an effective catalyst for the synthesis of DMC via transesterification of EC and methanol,

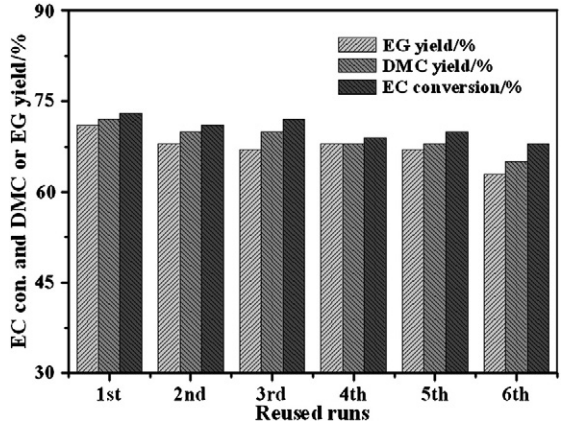


**Fig. 5.** Recycling tests for DMC synthesis from EC and methanol over $Zn_3Y$-400 catalyst. (Reaction conditions: EC, 30 mmol; Methanol, 240 mmol; Catalyst, 0.07 g; 2 h; 65 °C.).

corresponding to TOF of 236 mmol/$g_{cat}$ h. The order of the catalytic activity was essentially consistent with that of medium basic sites. Moreover, the catalytic activity can be regenerated after a simple calcination handling.

## References


[1] P. Tundo, M. Selva, Accounts of Chemical Research 35 (2002) 706.
[2] S. Fukuoka, M. Kawamura, K. Komiya, M. Tojo, H. Hachiya, K. Hasegawa, M. Aminaka, H. Okamoto, I. Fukawa, S. Konno, Green Chemistry 5 (2003) 497.
[3] S.P. Gupte, A.B. Shivarkar, R.V. Chaudhari, Chemical Communications 24 (2001) 2620.
[4] Y. Ono, Catalysis Today 35 (1997) 15.
[5] Y. Ono, Applied Catalysis A: General 155 (1997) 133.
[6] M.A. Pacheco, C.L. Marshall, Energy & Fuels 11 (1997) 2.
[7] T. Wei, M.H. Wang, W. Wei, Y.H. Han, B. Zhong, Green Chemistry 3 (2003) 343.
[8] H. Babad, A.G. Zeiler, Chemical Reviews 73 (1973) 75.
[9] D. Delledonne, F. Rivettia, U. Romano, Applied Catalysis A: General 221 (2001) 241.
[10] T. Sakakura, J.C. Choi, H. Yasuda, Chemical Reviews 107 (2007) 2365.
[11] W.L. Dai, S.L. Luo, S.F. Yin, C.T. Au, Applied Catalysis A: General 366 (2009) 2.
[12] M. North, R. Pasquale, C. Young, Green Chemistry 12 (2010) 1514.
[13] B.M. Bhanage, S.I. Fujita, Y. Ikushima, M. Arai, Applied Catalysis A: General 219 (2001) 259.
[14] J. Li, L. Wang, F. Shi, S. Liu, Y. He, L. Lu, X. Ma, Y. Deng, Catalysis Letters 141 (2011) 339.
[15] Y. Watanabe, T. Tatsumi, Microporous and Mesoporous Materials 22 (1998) 399.
[16] R. Srivastava, D. Srinivas, P. Ratnasamy, Journal of Catalysis 241 (2006) 34.
[17] B.M. Bhanage, S. Fujita, Y. He, Y. Ikushima, M. Shira, K. Torii, M. Arai, Catalysis Letters 83 (2002) 137.
[18] S.G. Liu, J. Ma, L.X. Guan, J.P. Li, W. Wei, Y.H. Sun, Microporous and Mesoporous Materials 117 (2009) 466.
[19] G. Stoica, S. Abello, J. Perez-Ramirez, ChemSusChem 2 (2009) 301.
[20] S.R. Jagtap, M.D. Bhor, B.M. Bhanage, Catalysis Communications 9 (2008) 1928.
[21] R. Juarez, A. Corma, H. Garcia, Green Chemistry 11 (2009) 949.
[22] S. Yan, M. Kim, S.O. Salley, N.K. Simon, Applied Catalysis A: General 360 (2009) 163.
[23] J. He, G.Q. Xie, J.Q. Lu, L. Qian, X.L. Zhang, P. Fang, Z.Y. Pu, M.F. Luo, Journal of Catalysis 253 (2008) 1.
[24] Y. Zhang, R.J. Puddephatt, Chemistry of Materials 11 (1999) 148–153.
[25] V.E. Henrich, P.A. Cox, The Surface Science of Metal Oxides, Cambridge University Press, Cambridge, 1994.
[26] X. Xie, W. Shen, Nanoscale 1 (2009) 50.
[27] U. Zavyalova, M. Geske, R. Horn, G. Weinberg, W. Frandsen, M. Schuster, R. Schlogl, ChemCatChem 3 (2011) 949.
[28] J. Otera, Chemical Reviews 93 (1993) 1449.